IMAGE RESOLUTION EFFECTS FOR VEGETATION MAPPING FROM LANDSAT 7 ETM+ AND TERRA MODIS DATA

Piero BOCCARDO[*], Enrico BORGOGNO MONDINO[*], Pierluigi CLAPS[**], Francesca PEREZ[*]

ABSTRACT

To evaluate accuracy of low resolution vegetation mapping for hydrological purposes, a comparative study of NDVI images derived from MODIS and Landsat 7 ETM+ data has been done. Main goal is to understand how effective MODIS images can be for vegetation characterization on large areas, as compared to the Landsat 7 ETM+ ones.

This paper presents:

a) a methodology aimed at measuring the difference between NDVI values derived from the two sources, considering synthetic parameters and investigating their dependency on the geometric resolution of the images. The proposed approach considers correspondences between the NDVI values computed in the MODIS pixel and statistics (e.g. mean value) extracted from the group of Landsat pixels belonging to the MODIS pixel polygons. In this comparison, a systematic bias was found, and corrected, in the computed MODIS NDVI

b) a new resampling method for MODIS NDVI imagery, that allows its spatial resolution to be improved by using geometric reference information obtained from a classification of the main land covers derived from Landsat ETM+ data. The basic idea is that the geometric clustering of the territory does not change over time, even though its radiometry does. It is therefore possible to consider using a single ETM+ classification map to drive a continuous resampling process of the MODIS NDVI time series to a better geometric resolution.

Some comparisons and tests are presented to demonstrate the added value of this approach in the exploitation of high frequency and low resolution satellite acquisitions (MODIS). In particular, NDVI images resampled to the geometric Landsat 7 ETM+ resolution and images obtained following the traditional approach (nearest neighbour) are compared, demonstrating the good performances of the resampling procedure.

* DITAG, Politecnico di Torino, Corso Duca degli Abruzzi 24, TORINO

**DITIC, Politecnico di Torino, Corso Duca degli Abruzzi 24, TORINO

1. RESEARCH GOAL

This study is part of a research project aimed at evaluating which limits and potentialities result from the use of low resolution MODIS data for hydrological purposes, in support to water balance studies in river basins with little available data. This is of great importance, for instance, in large areas of developing countries, where hydrological monitoring alone cannot allow comprehensive studies on long-term water balance. In this context, continuity of available data as guaranteed by the MODIS platform can be an important resource (see e.g. Gallo et al., 2005; Thome et al., 2003). If the areas of interest are of the order of a few hundreds of km^2 it is also important to have an evaluation of the quality of the MODIS representation of variables of hydrological interest, such as vegetation. A way to afford this task is to refer to higher resolution sensors in a coarse-resolution approach (see e.g. Oleson et al, 1995). For instance, in comparison with Landsat 7 data, a wider use of MODIS can be considered a sensitive matter also:

- because of the currently operational limitations of Landsat 7 (slc-off acquisitions);
- because of the greater economic convenience of the MODIS data (that are free);
- because of the higher frequency of MODIS acquisition.

In particular, considering vegetation properties, the main task of this work is the comparison of NDVI images derived from Terra MODIS and Landsat 7 ETM+ data. In pursuing this goal, a methodology aimed at measuring the difference between NDVI values derived from the two different data and the result of a radiometric comparison are first presented. Subsequently, a new resampling method for MODIS NDVI images is described, based on geometric reference information obtained from other external data.

2. DATA AND TEST AREA

Two pairs of contemporary images, acquired by the sensors Terra - *MODIS* (*Moderate Resolution Imaging Spectrometer)* and Landsat 7 *ETM+* (*Enhanced Thematic Mapper*) respectively were considered in this work.

The test area is a portion of the northern coast of Sicily (Italy), as shown in Figure 1, that comprises the Belice Basin. This area was chosen mainly because of the great variety of vegetation and other land covers that can be encountered.

Considering MODIS images, the product named "*MODIS/Terra Calibrated Radiances 5-Min L1B Swath 250m*" (MOD02QKM) was selected for this study (Toller, 2003; Barbieri, 1997). Level 1B images represent calibrated and geolocated data for MODIS spectral bands 1 and 2. The MODIS data were obtained free of charge on the Web from the EDG (*EOS Data Gateway*).

As far as ETM+ images are concerned, ESA CEOS data were used for the study. Two datasets (each containing one MODIS and one ETM+ image) were prepared considering two similar

summer dates of different years (02/08/2000, 07/07/2002). The above datasets were forced to assume the same size in order to make the results comparable.

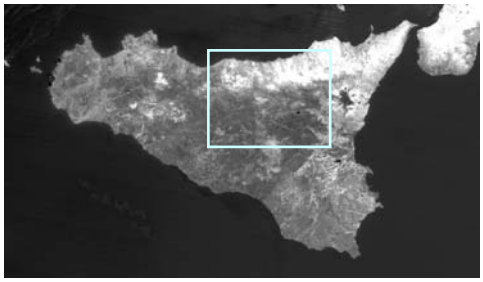

Figure 1 - Test area over Sicily (Italy).

The basic features of the two sets of data are shown in Table 1. From these data, 2 ETM+ and 2 MODIS images of the NDVI (*Normalized Difference Vegetation Index*) were derived:

$$NDVI = \frac{NIR - R}{NIR + R} \tag{1}$$

where: R = *Red band;*
NIR = *Near Infra-Red band.*

NDVI varies between -1 and + 1. Due to its 'ratioing' properties, NDVI cancels out a large proportion of signal variations attributed to calibration, noise, and changing irradiance conditions that accompany changing sun angles, topography, clouds/shadow and atmospheric conditions.

Table 1 - Basic features of MODIS and ETM+ data

	Terra-MODIS	**Landsat 7-ETM+**
Bandwidth specifications	*Band 1: 620-670nm* *Band 2: 841-876 nm*	*Band 3: 630-690 nm* *Band 4: 780-900 nm*
Spatial resolution	*250 m*	*30 m*
Radiometric resolution	*12 bits*	*8 bits*
Data Frequency	*2 days (global coverage)*	*16 days (seasonal global coverage capability)*

3. DATA COMPARISON PROCEDURE

3.1 IMAGE DATASET CO-REGISTRATION

In order to compare MODIS and Landsat NDVI values, the images were radiometrically preprocessed and co-registered in advance. The radiometric calibration of the Landsat data was carried out to convert sensor DNs (*Digital Numbers*) to at-sensor reflectances; the atmospheric correction was successively performed for both data through the simplified Dark Subtraction approach. Solar and topographic correction was ignored since NDVI is a ratio in which multiplying factors can be neglected.

Image co-registration was done following the procedure described in the Appendix. In fact, while evaluating, from an operational point of view, two different image sources (*MODIS* and *Landsat 7*) great attention has to be paid to their co-registration. It should be pointed out that by co-registered images we intend geometrically coherent images, whose pixels are homologous to each other. Any consideration about image radiometry is greatly conditioned by the "goodness" of such an operation.

The comparison procedure operates by calculating the correspondent floating point Landsat image coordinates for the 4 corners of each MODIS pixel.

For each MODIS pixel can be therefore defined a polygon ($P_{landsat}$) in the Landsat space, that includes several Landsat pixels (Figure 2). These pixels are considered to contribute to the total reflectance which is recorded as a single value by the MODIS CCD (*Charge Coupled Device*). The comparison proceeds considering the statistical features of the DN of these Landsat pixels with the single DN obtained from the original homologous MODIS pixel.

3.2 SPECTRAL COMPARISON

The NDVI comparison was carried out according to the following two steps:

a) the first step (statistical analysis) was devoted to the quantification of the local differences between the NDVI values;

b) the second step was devoted to the assessment of the nature of the resulting NDVI differences and to the identification of the MODIS pixels that can be considered "critical" (i.e. those for which the underlying Landsat image would produce corrections). Features related to the radiometric homogeneity inside the MODIS pixels were investigated in particular.

3.2.1 Statistical analysis of NDVI differences

NDVI Landsat pixels that belong to the $P_{Landsat}$ polygon were represented by synthetic parameters that can allow the comparison to be made. Sensor recording mode suggested the

choice. During the acquisition process, the sensors integrate the radiation from the ground area defined by the IFOV (*Istantaneous Field of View*) and code it as a single discrete value (DN). This can therefore be considered as the result of the sum of energy reflected by all the objects that belong to the IFOV area; these objects participate in the signal, according to their different spatial distribution inside the IFOV area itself. This would suggest to calculate, for each $P_{Landsat}$ polygon, some parameters suitable to describe the global spectral behaviour of the pixels included in the polygon. The considered parameters are: mean μ_{NDVI_L}, median Md_{NDVI_L} and standard deviation σ_{NDVI_L} of the NDVI values. A first analysis was carried out to verify the possible existence of a relationship between the MODIS NDVI values (single pixels) and the mean Landsat NDVI values calculated for each $P_{Landsat}$. The *Pearson linear correlation coefficient, Rx,y,* was therefore calculated. The $R_{X,Y}$ values are $\geq$ 0.9 for both the considered datasets (2000 and 2002), demonstrating the existence of a relationship between the two populations.

This was a basic condition and requirement for the subsequent tests.

In order to quantify the NDVI differences for each dataset, the following deviations were calculated:

$$\begin{aligned} \Delta_{LM_1} &= \mu_{NDVI_L} - NDVI_M \\ \Delta_{LM_2} &= Md_{NDVI_L} - NDVI_M \end{aligned} \qquad (2)$$

where: $NDVI_M$ = MODIS NDVI value for generic pixel i;
μ_{NDVI_L}, Md_{NDVI_L} = mean and median values calculated for the corresponding $P_{Landsat}$.

The concept underlying the computation of NDVI deviations is illustrated in Figure 2.

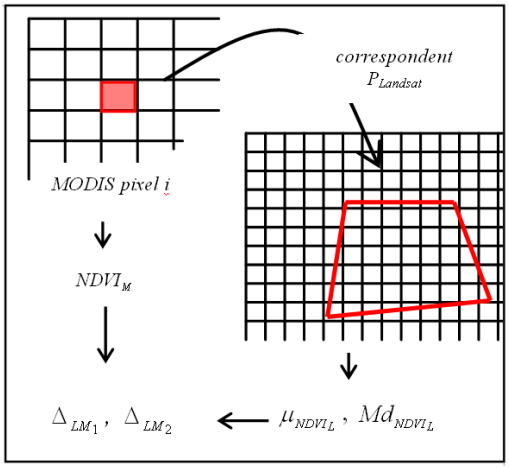

Figure 2 - NDVI difference (Δ_{LM}) computation scheme based on the polygon approach.

Taking into account the kind of vegetation that covers the quite arid area under study, it was assumed sufficient to consider the range of NDVI values (related to the Landsat data) between -0.2 and 0.8. A total of 20 $NDVI_L$ classes of width equal to 0.05 were identified within this range. For each $P_{Landsat}$ the difference Δ_{LM} was assigned to the $NDVI_L$ class to which μ_{NDVI_L} was associated.

The mean $\overline{\Delta_{LM\ i}}$ of the obtained deviations was calculated for each class. $\overline{\Delta_{LM\ i}}$ values obtained indicate that MODIS NDVI values are higher than the ETM+ ones for the two observation years. Other works confirm this general trend in the data (Buheaosier et al., 2003). Figure 3 shows that the deviations $\overline{\Delta_{LM\ i}}$ are correlated to the values of the $NDVI_L$ classes for the two observation periods. The relationship between the two observed variables can be approximated (at least for $NDVI_L$ values > -0.25) with linear functions with almost the same slope (see Figure 3).

It is worth to underline that linear regression parameters estimation was conducted without taking care of the number of observations of each NDVI class, in order to generate a correction tool suitable for all the NDVI values.

Further research is at present performed with the aim of verefying whether these observed systematic differences can be related to specific critical states of the calibration algorithms used by the distributors of MODIS imagery, or to some limits of the applied simplified atmospheric correction models.

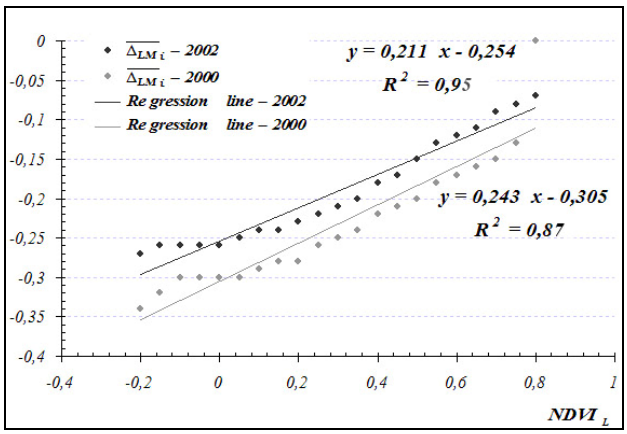

Figure 3 - Trends of the deviation means $\overline{\Delta_{LM\ i}}$ respect to $NDVI_L$ value for the two observation periods and pertinent interpolation lines.

The identification of linear relationships allowed the observed bias from NDVI MODIS image to be removed. This was necessary for the evaluation of the residual differences which were

closely connected to the different *Ground Sample Distance* (GSD) of the two types of data. This correction (matrix operation over the NDVI MODIS image) was applied as follows:

$$MOD = NDVI_M + C_{NDVI} \tag{5}$$

where: $NDVI_M$ = MODIS NDVI value for pixel *i*;
C_{NDVI} = correction value estimated by linear regression.

Using the corrected NDVI MODIS images (MOD), new deviations, as in (2) were calculated between the NDVI values. The distribution of the obtained deviations was again analysed respect to the previous $NDVI_L$ classes. The new results are illustrated in Figure 4 and 5.

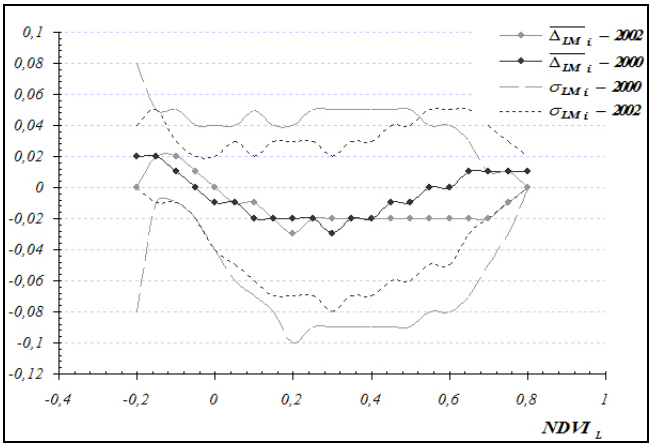

Figure 4 - Trends of the new deviations $\overline{\Delta_{LM\,i}} \pm \sigma_{LM\,i}$ *with respect to* $NDVI_L$ *values for the two observation periods.*

Figure 4 shows that deviations now range around zero, without any further systematic bias. Furthermore, the observed differences settle on values that are much lower than the corresponding standard deviations $(\sigma_{LM\,i})$. Figure 5 shows how deviations are distributed in frequency with respect to the considered $\overline{\Delta_{LM\,i}}$ classes.

3.2.2 Critical MODIS pixel mapping

The possible source of the deviations emerged during the previous step was investigated considering the radiometric homogeneity of the $P_{Landsat}$ corresponding to the MODIS pixels. In particular, the distribution of the NDVI Landsat values of each $P_{Landsat}$ pixel was analysed to verefy whether one of the following characteristic situations could occur:

- The pixels belonging to $P_{Landsat}$ have a mean value μ_{NDVI_L} that falls into the class of NDVI to which the absolute majority (> 50%) of the pixels of $P_{Landsat}$ belongs. These MODIS pixels are characterised by radiometric homogeneity. Small NDVI deviations are expected for this type of polygons (hereafter referred to as *Type A* pixels);
- the mean value μ_{NDVI_L} is a result of the joint contribution of groups of pixels belonging to different NDVI classes, none of which represents the absolute majority (see e.g. the frequency distribution in Figure 6). The corresponding MODIS pixels are mixed and represent the cases in which the different geometric resolutions of the two sensors produce different results. These MODIS pixels are hereafter referred to as *Type B* or "mixed".
- the mean value μ_{NDVI_L} falls into a NDVI class different from that to which the absolute majority (> 50%) of the pixels of the $P_{Landsat}$ belong. In this case, we are dealing with MODIS pixels whose measure has to be verefied (hereafter referred to as *Type C* pixels).

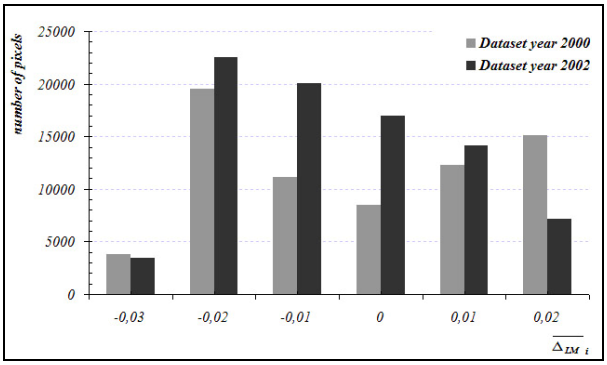

Figure 5 - Distributions of $\overline{\Delta_{LM\ i}}$ for the datasets relative to the years 2000 and 2002. It can be noticed that some classes result to be more numerous than the others. In particular MODIS derived NDVI values seem to mainly overestimate the signal if compared to the Landsat derived ones (negative deviations).

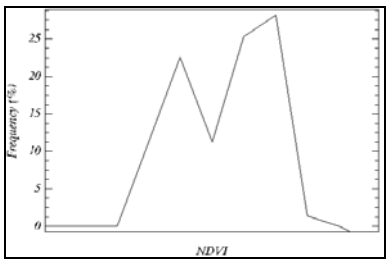

Figure 6 - Relative frequencies in a $P_{Landsat}$ type B polygon.

The previously illustrated conditions were verefied considering a range of $NDVI_L$ values between -0.2 and +0.8 (0.1 amplitude classes). According to the above definitions, each MODIS pixel vas assigned to one of the three previously defined classes (A, B or C) and MODIS classified images were generated corresponding to the two investigated periods.

The results obtained after the subdivision in the 3 types of classes is summarised in Figure 7. As it can be seen, *Type A* MODIS pixels prevail in the dataset relative to the year 2002, while *Type B* MODIS pixels prevail in the dataset relative to the year 2000. The *Type C* pixels seem to have a similar incidence for both the images. This information can be used to estimate the potential "expected" error that can be ascribed to the adoption of the MODIS data instead of the Landsat one. *Type B* pixels are those on which most efforts must be concentrated.

A joint analysis has made it possible to evaluate the existence of a relationship between the distribution of the deviations Δ_{LM} and the typology of the MODIS pixels. The graphs shown in Figure 8 and 9 illustrate the Δ_{LM} frequency distribution for the three considered types. The data summarised in the diagrams refer to the complete datasets, including the pixels with values of NDVI outside the considered range.

It can be seen that for the majority of cases the deviations have a maximum frequency (mode) in correspondence to values close to zero for all the types of pixels examined. A prevalence of *Type A* MODIS (or homogeneous) pixels can be observed for the smaller absolute deviations, as expected. Correspondingly, the contribution to the total distribution given by the *Type B* pixels becomes more important for the higher values of the deviations Δ_{LM} .

According to the purposes of vegetation characterisation of the territory useful for hydrological applications, a critical value of $|\Delta_{LM}| > 0.1$ was considered for the deviations, to investigate the homogeneity of the MODIS pixels exceeding a give threshold. The results of these analyses are given in Table 2.

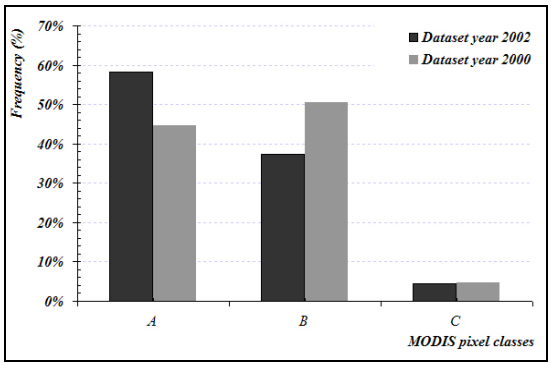

Figure 7 – Relative frequency of the three types of MODIS pixels relative to the examined datasets.

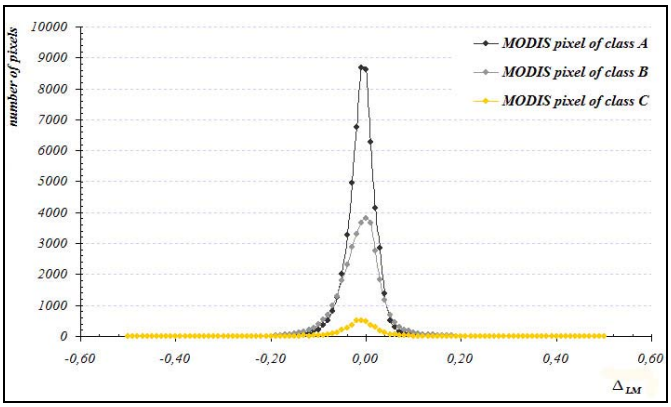

Figure 8 – Frequency distributions of Δ_{LM} for the 2002 dataset.

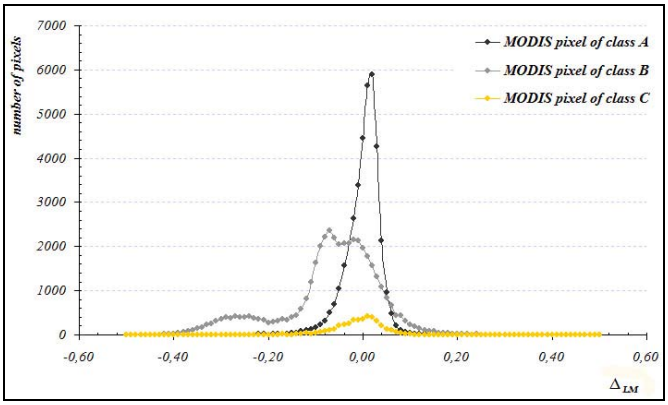

Figure 9 - Frequency distribution of Δ_{LM} for the 2000 dataset.

As it can be seen, the critical MODIS pixels represent a relatively small percentage of the total scene. It can also be observed that the critical deviations are prevailingly related to the presence of *Type B* MODIS pixels. On the other hand, not all *type B* pixels present critical deviations (see *e.g.* figure 8). Additional images are required to better investigate relations between error amounts and frequency distribution of Landsat pixels within MODIS polygons.

The spatial distribution of the critical MODIS pixels ($|\Delta_{LM}| > 0.1$) is represented in the MODIS image of Figure 10.

Table 2 - Distribution of critical MODIS pixel types.

2000	Pixels with $\|\Delta_{LM}\| > 0.1$	14.25% of the total (84240 pixels)	type A type B type C	5.33% 92.92% 1.75%	639 pixels 11156 pixels 211 pixels
	Pixels with $\|\Delta_{LM}\| < 0.1$	85.75% of the total (84240 pixels)	type A type B type C	51.04% 43.59% 5.36%	
2002	Pixels with $\|\Delta_{LM}\| > 0.1$	2.64% of the total (92697 pixels)	type A type B type C	30.60% 62.68% 6.73%	749 pixels 1535 pixels 165 pixels
	Pixels with $\|\Delta_{LM}\| < 0.1$	97.36% of the total (92697 pixels)	type A type B type C	59.07% 36.64% 4.29%	

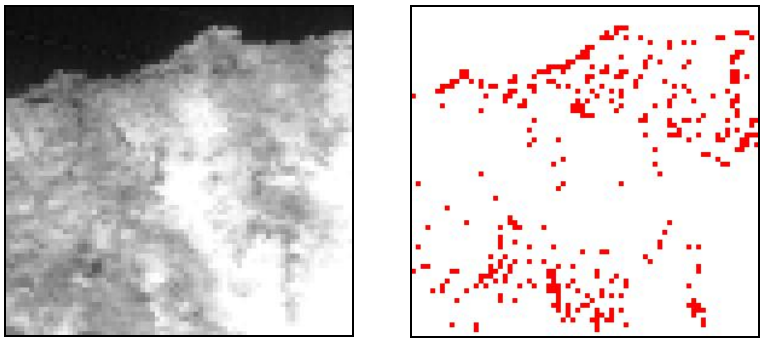

Figure 10 - MODIS critical pixels $|\Delta_{LM}| > 0.1$ mapped over the scene (an example subset).

4. A NEW RESAMPLING METHOD OF MODIS NDVI IMAGES BASED ON INTEGRATION WITH LANDSAT 7 ETM+ DATA

It was stated previously that time series of MODIS imagery provide almost real time, continuous, and free data, but their relatively coarse spatial resolution limit their exploitation for certain applications. To improve the possibility of following the evolution of NDVI during the year a new resampling method for MODIS NDVI imagery (supposed belonging to a time series) is proposed here. This is aimed at improving the MODIS spatial resolution making use of geometric reference information obtained from a classification map of the main land covers derived from Landsat ETM+ data. The basic idea is that the geometric clustering of the territory does not strictly

follows changes in its radiometric response; it is therefore possible to drive the resampling process of the MODIS NDVI time series to a better geometric resolution using a single ETM+ classification map.

4.1 OBJECTIVES

Th experimental procedure developed here to georeference and over-sample MODIS images has the following innovative peculiarities:

- the georeferencing process is of *downward* type (from the MODIS space down to the reference one) in which MODIS transformed pixels are assumed to be polygons containing pixels at a higher resolution;
- the over-sampling process from low to higher spatial resolution is driven by some geometric information derived from an available static land cover map (in the following called C_{ref} or *Reference Map*).

The goal is to geometrically solve the problem of the mixed pixels. The C_{ref}, in the proposed procedure, is represented by a raster dataset whose spatial resolution is equal to the one expected for the georeferenced over-sampled MODIS image. C_{ref} can be a simplified classification of territory land covers derived from other satellite datasets (as Landsat 7 ETM+ in the present case) or coming from other external sources (e.g. *CORINE* land cover map). Within the procedure, C_{ref} drives the radiometric resampling process of MODIS images exploiting some geometric discriminants. These are basically coincident with the border lines of the polygons defining the different areas with homogeneous land cover. Their task is to declare the spatial and semantic continuity of radiometry inside the single MODIS pixel in order to investigate what happens inside each low resolution pixel and to decide how to break it while resampling.

4.2 REFERENCE CLASSIFICATIONS

Two classifications were produced from the Landsat ETM+ NDVI images, by grouping NDVI values in accordance with progressive radiometric ranges (*Density Slicing*) for both the observation years (2000 and 2002). Their spatial resolution is the same as the original Landsat image: 30 metres. The entire range of existing NDVI values (-1 ÷ +1) was thus split into twenty 0.1 width classes. Figure 11 shows, for example, the obtained 2002 reference classification map.

These NDVI classifications were used as geometric reference data during the NDVI MODIS images resampling process.

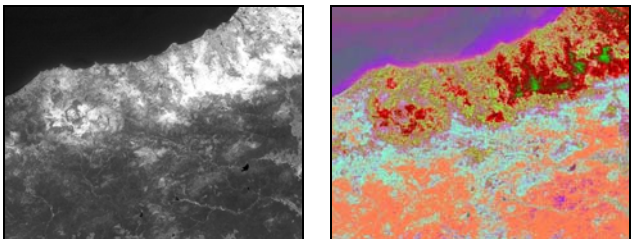

Figure 11 - 2002 NDVI Landsat ETM+ image (on the left) and the obtained classification of territory (on the right). In the classification image each colour corresponds to a different NDVI interval (0.1 wide).

4.3 GEOREFERENCING PROCEDURE

While dealing with image georeferencing two main issues have to be considered:

- the geometric model to adopt;
- the resampling method to use.

Usually the former issue directly conditions the resulting positioning accuracy of the georeferenced image, while the latter mainly influences the radiometric quality of the image and its interpretability.

4.3.1 The geometric model

When the images to be georeferenced (or co-registered) are characterized by a low geometric resolution (as the 250 m MODIS data is) it is common to adopt planar transformations to relate each other, admitting that the relief displacement and sensor model contribution to image deformations is negligible if compared to the pixel size. For such type of data, in fact, the collimation error during the Ground Control Points (GCPs) selection is the greatest. Anyway, while processing images where terrain height variation is quite high, it is suggested to proceed to a preliminary verefication of the potential error introduced, at least, by the relief displacement. A preliminary investigation of the potential relative error due to relief displacement was carried out (see chapter 3.1 and the Appendix). On the basis of the previous assessment, it was in fact decided that a preliminary image orthoprojection step had to be performed as it was demonstrated in the Appendix. If a single Landsat image is used as reference for a MODIS images time series, potential relative image deformations necessarily occur and they increase with the gap between the orbit paths of TERRA and Landsat 7 satellites.

4.3.2 Images co-registration

The proposed procedure has been developed in the IDL (*Interactive Data Language*) programming language. It is based on an image-to-image georeferencing approach (in the following called co-registration), in which the reference data (base image) is the C_{ref}. As far as this work is concerned, the case study refers to the processing of an NDVI image obtained from band 1-2 of MODIS (250 m spatial resolution). It is worth to remind that the declared goals are:

- to georeference the NDVI MODIS image (orthoprojected) respect to the C_{ref} ;
- to over-sample it at the spatial resolution of 30 m (same as C_{ref}) improving radiometric information.

The two related reference systems are therefore:

- the image reference system of the original corrected NDVI MODIS image (MOD, see 3.2.1);
- the reference system of C_{ref} (S_1).

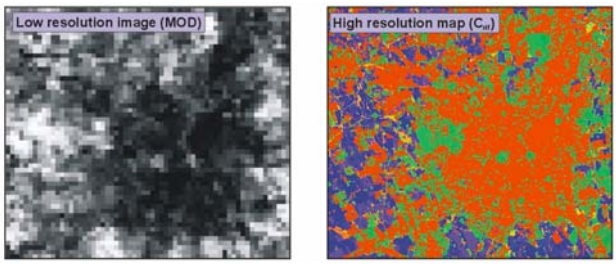

Figure 12 - Original NDVI MODIS image (a subset) and the correspondent high resolution reference map (on the right).

4.3.3 The resampling procedure

Considering the proposed co-registration downward approach (see the Appendix and chapter 3.1), if a traditional *Nearest Neighbour* resampling method was applied, it would fill all the pixels belonging to P_T with the DN coming from the single pixel MOD they correspond to. Considering that surfaces at the ground change their reflectance, but mostly preserve their shape (grass in a parcel changes, but parcel borders remain the same), it is possible to use geometric discontinuities (borderlines of polygons of the C_{ref}) to break those pixels that lay between two (or more) different homogeneous areas. In this way some high resolution pixels of the resampled image (in the following called *MODnew*) corresponding to the same MOD pixel can be filled with different DN (*Digital Number*).

The proposed resampling procedure follows two steps:

4.3.3.1 STEP 1

a. The *MODnew* image is initialized with the same size and spatial resolution as C_{ref}. It will contain the georeferenced and oversampled MODIS image;
b. for each pixel of the MOD image the correspondent polygon P_T is defined in S_1 through the projection of the four vertices of the starting MOD pixel;
c. the MOD pixel center (c_0) is projected in S_1 and the correspondent pixel of *MODnew* (within P_T) is filled with the DN of the starting MOD pixel;
d. a *Region Growing* process starts propagating the DN of c_0 to all the adiacent pixels of P_T that belong to the same class of c_0. A class check is done exploiting the information from C_{ref};
e. when no other adjacent pixels of P_T are found belonging to the same class of c_0, algorithm proceeds considering the successive MOD pixel. Not-filled pixels of P_T are labeled with the DN of the class they belong to, read from C_{ref}.

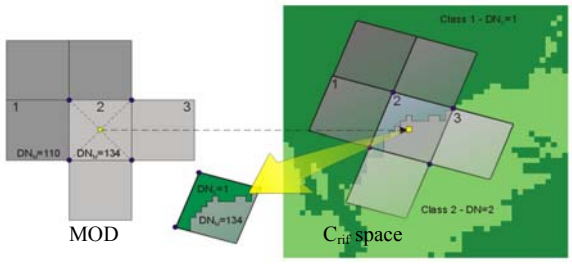

Figure 12 - Step 1 of the resampling procedure. Only some pixels of MODnew are filled considering a region growing process propagating the original DN from the pixel of P_T corresponding to the centre of the original MOD pixel. Region growing process cannot exceed the borders of P_T.

At the end of this step (Figure 12 and 14) *MODnew* is correctly georeferenced respect to C_{ref} and only partially filled. Filling completion is carried out during STEP 2 (Figure 13).

4.3.3.2 STEP 2

a. All the *MODnew* pixels that were not filled with a DN coming from the MOD image are identified;
b. a 3x3 window (k_R) centered over each of the identified not-filled pixels (P_i) is considered to investigate neighbourhood relationship between pixels;
c. the class of P_i (whose label was written in place of DN, C_i) is compared to the class of all the pixels belonging to k_R (information is derived from C_{ref}). All the pixels belonging to the same class as P_i and already filled with a DN are selected, if present;
d. to all the pixels of k_R belonging to C_i, and not yet filled, is assigned a DN calculated as the weighted mean (respect to the Euclidean distance to the considered pixel) of the DN of the

already filled pixels of k_R (as found in c.);

e. algorithm goes on, in this way, by iteration, trying to successively fill all the unfilled pixels of *MODnew*.

f. a check is performed in order to evaluate the degree of convergence of the filling procedure. If it becomes too slow, the remaining unfilled pixels are finally filled with the DN of the nearest neighbour already filled pixel of *MODnew*.

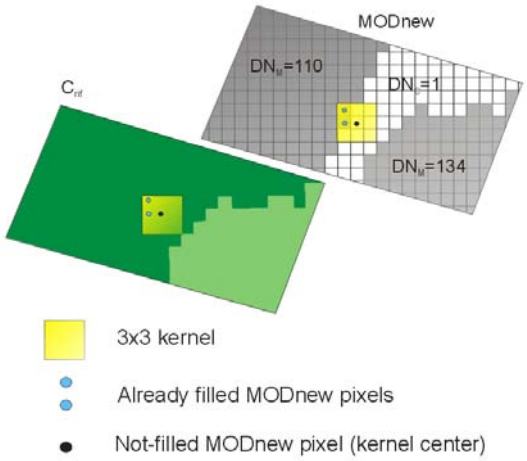

Figure 13 - Step 2 of the resampling procedure. Operating directly over MODnew all the unfilled pixels are filled through a neighbourhood analysis (3x3 kernel).

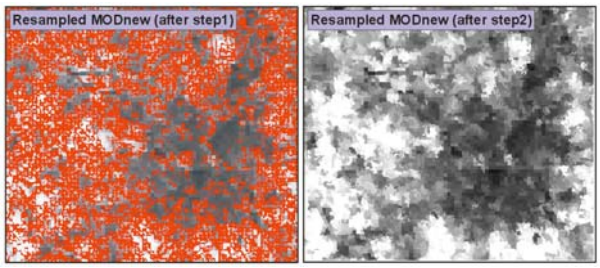

Figure 14 - MODnew after step 1 (on the left) and after step 2 (on the right). Red pixels on the left image indicate unfilled pixels at the end of step 1.

4.4 QUALITATIVE PERFORMANCE EVALUATION

In order to give a preliminary evaluation of the obtained resampled images (that will be hereafter referred to as $NDVI'_M$), a double comparison was made with:

1) NDVI images derived by the original Landsat ETM+ data (see 4.2; these images shall hereafter be known as $NDVI_L$);
2) NDVI MODIS images resampled through two procedures based on a *Nearest Neighbour* approach:
   2.a) a co-registration downward procedure equal to that presented in this work, but which does not use auxiliary geometrical information to determine DN of *MODnew*;
   2.b) a traditional upward type procedure.

The 2.a) resampling procedure shares the first two operations relative to step 1 with the innovative proposed procedure. For each pixel of the original NVDI MODIS, the corresponding P_T is identified in the space of the *MODnew* and all the pixels belonging to the P_T are filled with the same DN as the starting MOD pixel. The images resampled with this technique will be hereafter referred to as $NDVI''_M$.

Procedure 2.b) was carried out with the purpose of warping images with procedures similar to the ones usually available in the main commercial software (based on the *Nearest Neighbour* resampling method). This procedure was specifically set up by the authors to guarantee the utilisation of the same type of transformation (*f*) adopted in the other techniques considered in this study, as 2D rational polynomial does not exist in commercial software.

The resampled images, obtained using the two previously described procedures (2.a and 2.b), were compared to each other.

The results of this comparison led us to believe the $NDVI''_M$ resampled images can well approximate those obtained using the traditional resampling procedure (upward). This demonstrates that the downward approach is robust and the $NDVI''_M$ image can certainly be used as reference data during comparison with the $NDVI'_M$ images.

Some details taken from the $NDVI'_M$ resampled images and the corresponding areas extracted from the data used for comparison purposes ($NDVI_L$ and $NDVI''_M$ images) can be seen in Figures 15 and 16. These figures show that, with respect to the other techniques ($NDVI''_M$), a better interpretability of the territory shapes can be achieved with the images resampled with the proposed innovative procedure ($NDVI'_M$).

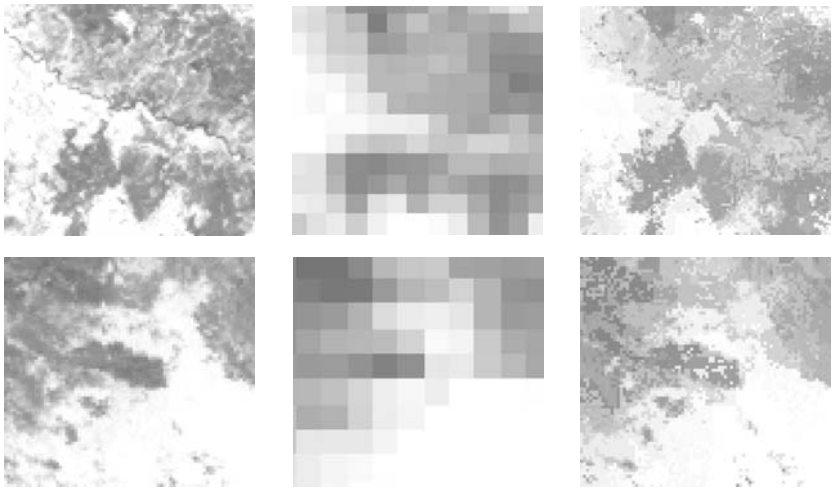

Figure 15 - Details extracted from the $NDVI_L$ images (on the left), the $NDVI''_M$ images (in the centre) and the $NDVI'_M$ images (on the right). Year 2000 dataset.

4.5 QUANTITATIVE PERFORMANCE EVALUATION

4.5.1 Validation based on comparison with Landsat ETM+ NDVI data (difference analysis)

The following matrix differences were defined in order to give a quantatitive evaluation of the improvement (or degradation) produced by the resampled $NDVI'_M$ data:

$$\begin{aligned} \Delta'_{ric} &= NDVI_L - NDVI'_M \\ \Delta''_{ric} &= NDVI_L - NDVI''_M . \end{aligned} \tag{6}$$

Differences were calculated for both the images. It is worth reminding that the $NDVI'_M$ and $NDVI''_M$ images obtained for each dataset result to be dimensionally equivalent and geometrically super imposable.

The distributions of the obtained image differences ($\Delta'_{ric}, \Delta''_{ric}$) showed comparable mean and standard deviations. This demonstrates that the proposed resampling procedure does not alter the radiometry of the original NDVI MODIS data more than the traditional resampling methods. Considering the previously defined critical threshold for the differences ($|\Delta| > 0.1$), pixels showing differences greater than the defined threshold were identified. The resulting percentage values are synthesized in Table 3, where it can be seen that the proposed resampling procedure reduces significantly the presence of critical difference values. A direct comparison of the performances of the two resampling procedures is presented in Table 4, which is self-explaining.

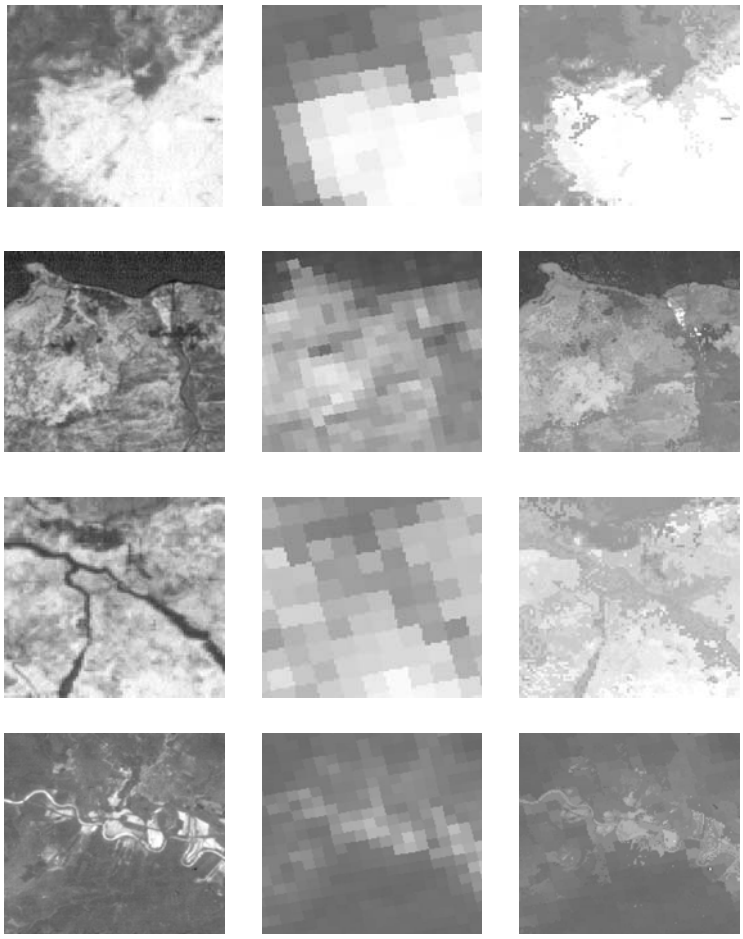

Figure 16 - Details extracted from the $NDVI_L$ images (on the left), the $NDVI''_M$ images (in the centre) and the $NDVI'_M$ images (on the right). Year 2002 dataset..

Both the images resampled by the proposed procedure present an improvement over the images resampled with traditional procedures. As can be seen in Table 4, this improvement is equal to 6.36 % of the total number of cells of the considered MODIS resampled image for the year 2000 and equal to 6.92 % for the year 2002.

Finally, for each resampled image, it was investigated how better the other one behaves in correspondence of those pixels that present greater differences with the reference datum.

The following distributions were taken into consideration:

- distributions of differences Δ'_{ric} for pixels in which $|\Delta'_{ric}| > |\Delta''_{ric}|$
- distributions of differences Δ''_{ric} for pixels in which $|\Delta'_{ric}| < |\Delta''_{ric}|$.

Results of this analysis are given in Table 5.

Table 3 – Distribution of the critical difference values for the resampled images. All percentages refer to the total number of pixels of the images (sea and scene border areas were excluded by masking).

2000	Pixels with $\|\Delta'_{ric}\| > 0.1$	19.94%
	Pixels with $\|\Delta''_{ric}\| > 0.1$	22.95%
2002	Pixels with $\|\Delta'_{ric}\| > 0.1$	11.78%
	Pixels with $\|\Delta''_{ric}\| > 0.1$	15.72%

Table 4 - Distribution of the values of the $\Delta'_{ric}, \Delta''_{ric}$ differences for the resampled images. All percentages refer to the total number of pixels of the images (sea and scene border areas were excluded by masking).

2000	Pixels in which: $\Delta'_{ric} = \Delta''_{ric}$	61.5%
	Pixels in which: $\|\Delta'_{ric}\| > \|\Delta''_{ric}\|$	16.07 %
	Pixels in which: $\|\Delta'_{ric}\| < \|\Delta''_{ric}\|$	22.43%
2002	Pixels in which: $\Delta'_{ric} = \Delta''_{ric}$	69.8 %
	Pixels in which: $\|\Delta'_{ric}\| > \|\Delta''_{ric}\|$	11.64 %
	Pixels in which: $\|\Delta'_{ric}\| < \|\Delta''_{ric}\|$	18.56 %

Data summarized in Table 5 demonstrate that, where $NDVI'_M$ behaves worse than $NDVI''_M$, resulting differences (Δ'_{ric}) are generally lower than the (Δ''_{ric}) obtained for $NDVI''_M$ where it behaves worse than $NDVI'_M$. This suggests that the NDVI approximation introduced by the proposed resampling method is better than the one introduced by a traditional approach.

4.5.2 Back-resampling validation

A new MODIS image (hereafter referred to as MOD') with spatial resolution of 250m was obtained, starting from the $NDVI'_M$ resampled images, by means of the proposed co-registration approach in backward mode. For each pixel of the original NVDI MODIS image (known as MOD), the corresponding P_T was identified in the space of the $NDVI'_M$ (NDVI MODIS resampled image, with spatial resolution of 30m) and the mean value of all the pixels belonging to the P_T was used to fill the correspondent pixel of the MOD' image.

Table 5. Distribution of the values of the differences $\Delta'_{ric}, \Delta''_{ric}$ for the resampled images. The percentages all refer to the number of pixels for which $|\Delta'_{ric}| > |\Delta''_{ric}|$ or $|\Delta'_{ric}| < |\Delta''_{ric}|$ (sea and scene border areas were excluded by masking).

		Mean	***StDev***	***% of pixels with $\|\Delta\|$ < 0.1***
2000	Differences Δ'_{ric} for pixels in which $\|\Delta'_{ric}\| > \|\Delta''_{ric}\|$	0.133	0.075	44.27%
	Differences Δ''_{ric} for pixels in which $\|\Delta'_{ric}\| < \|\Delta''_{ric}\|$	0.145	0.083	38.83%
2002	Differences Δ'_{ric} for pixels in which $\|\Delta'_{ric}\| > \|\Delta''_{ric}\|$	0.107	0.053	55.94%
	Differences Δ''_{ric} for pixels in which $\|\Delta'_{ric}\| < \|\Delta''_{ric}\|$	0.117	0.059	49.86%

The following matrix difference was calculated for the two considered datasets:

$$\Delta'_M = MOD' - MOD$$

The main features of the obtained Δ'_M distributions are given in Table 6.

Table 6. Distribution of the values of the Δ'_M differences (sea and scene border areas were excluded by masking).

	Mean	***StDev***
2000	0.023	0.029
2002	0.015	0.019

Results suggest that the resampling procedure seems to work well, following the real geometry of the land cover classes used as reference data, because this approach reproduces the MODIS sensor behaviour when it acquires radiance by integrating the signals coming from different surfaces, generating a mean radiance value.

6. CONCLUSIONS AND FUTURE DEVELOPMENTS

The analyses carried out on two different-resolution image pairs were addressed to the determination of the representativeness of MODIS-derived NDVI maps in place of the higher-

resolution Landsat NDVI. Main results obtained are as follows:

- the NDVI images derived from the MODIS acquisitions show a systematic difference (bias) with respect to the corresponding Landsat images; this bias has been corrected, but more information is needed to understand the nature of the problem;
- After the above-mentioned systematic correction, deviations between the two types of NDVI data were considered, to investigate the degree of representativeness of the 'bundled' MODIS value. Greatest deviations were recognized in 'mixed' cells (*Type B*), that contain heterogeneous NDVI classes. Limited cases of bi-modal distributions were found as sources of error.
- a non-negligible number of *Type B* pixels show error values lower than a 'critical' threshold of 0.1.

The comparison between the two types of data is greatly conditioned by the type of co-registration approach that is adopted. It can be considered that the proposed procedure guarantees a sufficient homology between the compared scenes, certainly higher than the one obtainable using simple planar transformations. According to the above results, we intend to proceed with a more detailed investigation of the systematic difference between MODIS and Landsat NDVI: many other case studies have to be considered before such a problem can be defined as "typical".

It would be interesting, furthermore, to look at the impact of the Point Spread Function in the bias found on NDVI.

To allow practical use of the above analyses, an innovative procedure for resampling NDVI MODIS images has been developed, based on geometric discriminants obtained from external data (e.g. from the classification of satellite images with greater geometric resolution). Results show that the produced resampled images guarantee a greater capacity of recognition of the shapes and geometric features within a scene, improving territory interpretability.

The tests performed on the radiometric contents of the resampled images seem to be promising, even though further validation is required. In particular the time persistence of shapes that drive the resampling procedure must be investigated, in order to correctly define how confidently the 'singularity' shapes can be used on seasonal or yearly basis).

Finally, the possibility to get auxiliary geometric information both from *CORINE* land cover data (*CORINE Land Cover*, 2000) and from all Landsat 7 bands is under test, to improve the building of classification maps .

6. ACKNOWLEDGEMENTS

This work has been supported by funds from Italian Ministry of Education and Research (MIUR COFIN 2003). Thanks are due to Goffredo La Loggia for providing the Landsat data.

7. REFERENCES

Barbieri R., Montgomery H., Qiu S., Barnes B., MODIS Level 1B Algorithm Theoretical Basis Document, MCST (MODIS Characterization Support Team) Algorithm Development Team, 1997.

Boccardo P., Borgogno Mondino E., Giulio Tonolo F., Lingua F. (2004), Orthorectification of high resolution satellite images, XX ISPRS Congress, Vol. XXXV part B1, ISSN 1682-1750, pp. 30-35, Istanbul (Turkey), July 2004.

Borgogno Mondino E., Gianinetto M., Giulio Tonolo F., Scaioni M. (2004), Satellite images geometric correction based on non-parametric algorithms and self-extracted GCPs, IGARSS 2004, Anchorage Alaska (USA), September 2004 (Proceedings on CD).

Buheaosier, Tsuchya K., Kaneko M., Sung S.J., Comparison of image data acquired with AVHRR, MODIS, ETM+ and ASTER over Hokkaido, Japan, Adv. Space Res. Vol. 32, No. 11, pp. 2211-2216, 2003.

Gallo K., Lei Ji, Reed B., Eidenshink J., Dwyer J., Multi-platform comparisons of MODIS and AVHRR normalized difference vegetation index data, Remote Sensing of Environment 99, 2005, pp. 221 – 231.

Thome K. J., Barnes R. A., Feldman G. C., Intercomparison of ETM+, MODIS, and SeaWiFS using a land test site, Proceedings of SPIE, Volume 4881 - Sensors, Systems, and Next-Generation Satellites VI, Hiroyuki Fujisada, Joan B. Lurie, Michelle L. Aten, Konradin Weber, Editors, April 2003, pp. 319-326.

Oleson, K.W., S. Sarlin, J. Garrison, S. Smith, J.L. Privette, and W.J. Emery, Unmixing multiple land-cover type reflectances from coarse spatial resolution satellite data, Remote Sensing of Environment 54, 1995, pp. 98-112.

Toller G.N., Isaacman A., MODIS Level 1B Product User's Guide, MCST (MODIS Characterization Support Team) for NASA/Goddard Space Flight Centre Greenbelt, 2003.

APPENDIX

IMAGE CO-REGISTRATION

The basic idea is to find a suitable relationship between the Landsat 7 sample grid and the MODIS one, in order to understand and measure the resulting differences. Even though the Landsat 7 and Terra satellite orbits are the same, the images acquired by ETM+ and MODIS sensors appear to be quite different, geometrically speaking; it is not an easy task to force one image to perfectly fit the other one. In order to reach an appropriate degree of correspondence, this problem was considered in great detail. Firstly, a preliminary evaluation of the relative positioning error (*RPE*) due to the relief displacement problem (the test area presents relief heights ranging from about 0 up to 1800 m) was carried out, following the operational scheme of *Figure 1.A*.

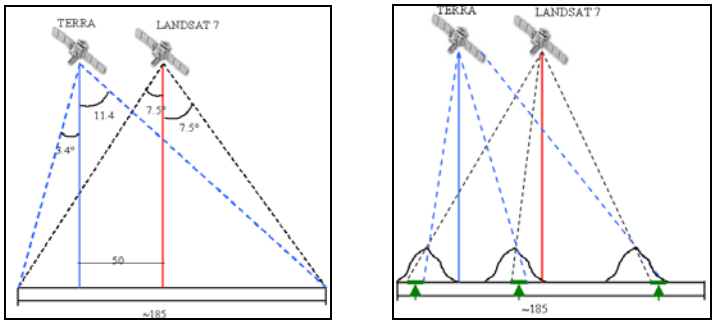

Figure 1.A - (Left) Satellite acquisition scheme; (Right) Relative Positioning Error variation over the scene (Landsat 7 image swath) due to relief displacement.

The mean distance between the satellite ground tracks were estimated to be about 50 km, according to the footprints of the images, as communicated by the metadata files.

Considering the size of the Landsat 7 image footprint, the correspondent RPEs were evaluated for different height values (H = 2000, 1000, 500 m). The results shown in *Table 1.A* demonstrate that a simple approach based on a flat image-to-image transformation cannot be adopted to co-register images.

An orthocorrection process was therefore carried out for both images to keep co-registration errors low.

A Digital Elevation Model with a 50 m grid step and an estimated height accuracy of about 2.5 m was used to produce orthoimages. 10 Ground Control Points (GCPs), extracted from a vector map (scale 1:25:000) of the Sicily coastline were used to assign a National Reference System to the image (ED 50 UTM 32N).

Table 1.A - RPEs vs Height values

Height (m)	**RPE min (m)**	**RPE min (n. pixel Landsat)**	**RPE max (m)**	**RPE max (n. pixel Landsat)**
2000	*141*	*4.7*	*162*	*5.4*
1000	*70*	*2.3*	*81*	*2.7*
500	*35*	*1.2*	*41*	*1.4*

The Landsat 7 images were corrected using OrthoEngine PCI Geomatics 9.0 software which is equipped with the rigorous Landsat model. The final orthoimages (2000 and 2002) estimated accuracy is about 0.7 Landsat pixels (that is, about 20 meters) according to the calculated Root Mean Square Error (RMSE) for both images.

MODIS bands 1 and 2 were corrected through a 1st order Rational Function Model (RFM, Boccardo et al., 2004; Borgogno Mondino et al., 2004). The resulting RMSE was about 0.45 MODIS pixels (that is, about 112 m) for both the 2000 and 2002 images.

In order to guarantee a better co-registration between the images, a further image-to-image registration procedure was applied to the obtained orthoimages. Some tests showed that the usual flat correction models (polynomials, triangulation, spline) were not sufficiently good, generating RMSE of about 4 Landsat pixels.

This has forced the authors to develop a specific routine for the task. A 2D rational polynomial transformation (HT1) was implemented (*IDL, Interactive Data Language* programming tool) relating the Landsat image coordinates (base image) to the MODIS one (warp image), according to the following relations:

$$c_L = \frac{A_1 \cdot c_M + A_2 \cdot r_M + A_3}{A_4 \cdot c_M + A_5 \cdot r_M + 1}$$
$$r_L = \frac{A_6 \cdot c_M + A_7 \cdot r_M + A_8}{A_9 \cdot c_M + A_{10} \cdot r_M + 1} \qquad (1.A)$$

where: A_i = model parameters
c_L, r_L = Landsat image coordinates
c_M, r_M = MODIS image coordinates.

Due to the great difference between the geometric resolution of the two types of data, there was a great uncertainty in the identification of suitable Ground Control Points, especially over the MODIS image, where the exact point correspondent to the one collimated over the Landsat image (30 m resolution) can float inside a larger window (the MODIS pixel).

In order to reduce this effect over the HT1 RMSE, considering that the implemented HT1 is calibrated using sub-pixel image coordinates, a specific collimation refining procedure was developed and applied before HT1. This procedure estimates the inverse HT (HT2) relating the MODIS image coordinates (base image) to the Landsat ones (warp image), (*equation 2.A*).

According to the residuals obtained from the Least Squares HT2 model parameter estimation, decimal digits of the collimated MODIS image coordinates (c_M, r_M) are moved to lower the RMSE, while the Landsat image coordinates remain the same.

$$c_M = \frac{B_1 \cdot c_L + B_2 \cdot r_L + B_3}{B_4 \cdot c_L + B_5 \cdot r_L + 1}$$
$$r_M = \frac{B_6 \cdot c_M + B_7 \cdot r_M + B_8}{B_9 \cdot c_L + B_{10} \cdot r_L + 1} \qquad (2.A)$$

where: B_i = model parameters
c_L,r_L = Landsat image coordinates
c_M, r_M = MODIS image coordinates.

This operation produces new corrected MODIS image coordinates for the Ground Control Points, which are then used to estimate HT1 parameters. The computed RMSEs are shown in *Table 2.A* and they represent the final co-registration errors that were accepted.

Table 2.A - RMSEs obtained after co-registration for the two datasets.

2000 dataset RMSE (Landsat pixels)	**2002 dataset RMSE (Landsat pixels)**
0.94	1.16

Figure 2.A shows how the proposed downward approach transforms the four corners of the original MODIS pixel into the correspondent image coordinates of the Landssat space (see chapter 3.1).

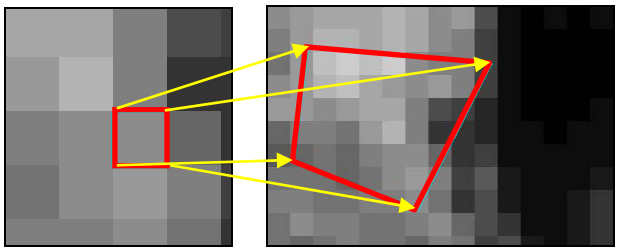

Figure 2.A - 2D rational polynomial model. The self-developed procedure operates by transforming the corners of each MODIS pixel into the Landsat image space. The result is a polygon containing some Landsat pixels.